

## Accepted Manuscript

Critical rainfall conditions for the initiation of torrential flows. Results from the Rebaixader catchment (Central Pyrenees)

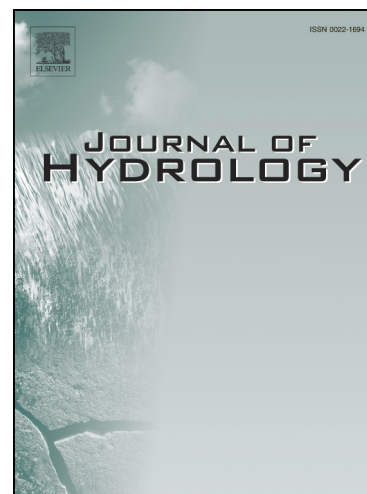
Clàudia Abancó, Marcel Hürlimann, José Moya, Marc Berenguer

PII: S0022-1694(16)00036-6

DOI: <http://dx.doi.org/10.1016/j.jhydrol.2016.01.019>

Reference: HYDROL 20977

To appear in: *Journal of Hydrology*



Please cite this article as: Abancó, C., Hürlimann, M., Moya, J., Berenguer, M., Critical rainfall conditions for the initiation of torrential flows. Results from the Rebaixader catchment (Central Pyrenees), *Journal of Hydrology* (2016), doi: <http://dx.doi.org/10.1016/j.jhydrol.2016.01.019>

This is a PDF file of an unedited manuscript that has been accepted for publication. As a service to our customers we are providing this early version of the manuscript. The manuscript will undergo copyediting, typesetting, and review of the resulting proof before it is published in its final form. Please note that during the production process errors may be discovered which could affect the content, and all legal disclaimers that apply to the journal pertain.

# Critical rainfall conditions for the initiation of torrential flows.

## Results from the Rebaixader catchment (Central Pyrenees)

Clàudia Abancó<sup>1,2</sup>, Marcel Hürlimann<sup>1</sup>, José Moya<sup>1</sup>, Marc Berenguer<sup>3</sup>

1 Division of Geotechnical Engineering and Geosciences; Department of Civil and Environmental Engineering, Technical University of Catalonia (UPC BarcelonaTech); claudia.abanco@upc.edu; marcel.hürlimann@upc.edu; jose.moya@upc.edu

2 Worldsensing S.L.

3 Center of Applied Research in Hydrometeorology (CRAHI-UPC); Technical University of Catalonia; marc.berenguer@crahi.upc.edu

Corresponding author: Clàudia Abancó (claudia.abanco@upc.edu)

### Abstract

Torrential flows like debris flows or debris floods are fast movements formed by a mix of water and different amounts of unsorted solid material. They generally occur in steep torrents and pose high risk in mountainous areas. Rainfall is their most common triggering factor and the analysis of the critical rainfall conditions is a fundamental research task. Due to their wide use in warning systems, rainfall thresholds for the triggering of torrential flows are an important outcome of such analysis and are empirically derived using data from past events.

In 2009, a monitoring system was installed in the Rebaixader catchment, Central Pyrenees (Spain). Since then, rainfall data of 25 torrential flows (“TRIG rainfalls”) were recorded, with a 5-minutes sampling frequency. Other 142 rainfalls that did not trigger torrential flows (“NonTRIG rainfalls”) were also collected and analysed. The goal of this work was threefold: i) characterize rainfall episodes in the Rebaixader catchment and compare rainfall data that triggered torrential flows and others that did not; ii) define and test Intensity-Duration (ID) thresholds using rainfall data measured inside the catchment by with different techniques; iii) analyse how the criterion used for defining the rainfall duration and the spatial variability of rainfall influences the value obtained for the thresholds.

The statistical analysis of the rainfall characteristics showed that the parameters that discriminate better the TRIG and NonTRIG rainfalls are the rainfall intensities, the mean rainfall and the total rainfall amount. The antecedent rainfall was not significantly different between TRIG and NonTRIG rainfalls, as it can be expected when the source material is very pervious (a sandy glacial soil in the study site). Thresholds were derived from data collected at one rain gauge located inside the catchment. Two different methods were applied to calculate the duration and intensity of rainfall: i) using total duration,  $D_{tot}$ , and mean intensity,  $I_{mean}$ , of the rainfall event, and ii) using floating durations,  $D$ , and intensities,  $I_{fl}$ , based on the maximum values over floating periods of different duration. The resulting thresholds are considerably different ( $I_{mean} = 13.20 D_{tot}^{-0.36}$  and  $I_{fl_{90\%}} = 5.49 D^{-0.75}$ , respectively) showing a strong dependence on the applied methodology.

On the other hand, the definition of the thresholds is affected by several types of uncertainties. Data from both rain gauges and weather radar were used to analyse the uncertainty associated with the spatial variability of the triggering rainfalls. The analysis indicates that the precipitation recorded by the nearby rain gauges can introduce major

uncertainties, especially for convective summer storms. Thus, incorporating radar rainfall can significantly improve the accuracy of the measured triggering rainfall.

Finally, thresholds were also derived according to three different criteria for the definition of the duration of the triggering rainfall: i) the duration until the peak intensity, ii) the duration until the end of the rainfall; and, iii) the duration until the trigger of the torrential flow. An important contribution of this work is the assessment of the threshold relationships obtained using the third definition of duration. Moreover, important differences are observed in the obtained thresholds, showing that ID relationships are significantly dependent on the applied methodology.

Keywords: rainfall thresholds, torrential flows, Pyrenees, rain gauges, weather radar

## Introduction

Torrential flows like debris flows, debris floods or hyperconcentrated flows consist of fast moving mixtures of water and different amounts of unsorted solid material. The definitions of these processes can be found in different publications such as Borga et al. (2014), Hungr et al. (2014) or Jakob and Hungr (2005). All these phenomena occur in steep torrents in mountainous regions and pose high risk for infrastructures and human settlements. Rainfall is the most common triggering factor (e.g. Wiczorek and Glade, 2005) and the analysis of the triggering rainfall conditions is a fundamental research task. Rainfall thresholds are an essential tool for: a) local and regional forecasting of natural hazards triggered by rainfall, and b) warning systems (Jakob et al., 2006; Badoux et al., 2009; Tiranti and Rabuffetti, 2010; Papa et al., 2013; Berenguer et al., 2015; Stähli et al., 2015). Therefore, the determination of rainfall thresholds is of particular interest.

Rainfall thresholds characterize the rainfall conditions that, when reached or exceeded, are likely to provoke one or more torrential flows (De Vita et al., 1998). There are two classes of thresholds: the physical or process-based ones, derived from models that simulate the infiltration and hydrologic behaviour of the rainfall over a susceptible soil layer (e.g. Crosta and Frattini, 2003; Godt et al., 2008; Papa et al., 2013), and the empirical ones, based on rainfall measurements from past events (e.g. Caine, 1980; Cepeda et al., 2010; Crozier and Glade, 1999). Regarding torrential flows like debris flows, rainfall thresholds have been established at different scales (Guzzetti et al., 2008) including regional studies covering large areas (Jibson, 1989; Wilson and Wieczorek, 1995; Jakob et al., 2012; Nikolopoulos, 2015) or specific studies referring to one single catchment (Deganutti et al., 2000; Badoux et al., 2009; Coe et al., 2008; Badoux et al., 2012).

Obtaining direct measurements of rainfall data near source areas in potential debris-flow basins is difficult. For this reason, many of the published thresholds for torrential flows have been established using data measured at the nearest rain gauges, often located several kilometers away from the initiation area of the torrential flows (Brunetti et al., 2010). Due to the intense convective behavior of the rainfalls that trigger torrential flows (with strong spatial and temporal variability), it is often difficult to precisely establish the real rainfall that triggers the event, and triggering rainfalls are many times underestimated (Abancó et al., 2012; Nikolopoulos et al., 2014; Restrepo et al., 2008).

Due to this important scale effect, thresholds established at regional, local or even catchment scale should be analysed separately. Generally, regional rainfall thresholds are defined for large areas up to several thousand square kilometers of similar climatological and physiographic characteristics. However, there is an important dependence of the thresholds on the site-specific conditions, so that, as it has been recently shown by Segoni et al. (2014a), a regional scale warning system is more

effective when the regional threshold is substituted with a combination of several site-specific local thresholds.

Some recent studies define thresholds for torrential flows at catchment scale, because the torrent has been monitored by different sensors including one or several rain gauges (Badoux et al., 2012; Coe et al., 2008; Cui et al., 2005; Deganutti et al., 2000). However, rainfall thresholds determined in monitored catchments are still very scarce.

The spatial variability of the triggering rainfall can be analysed based on weather radar observations. However, only very few cases have focused on the triggering conditions of torrential flows applying this technique (e.g. Marchi et al., 2009; Katzensteiner et al., 2012; Marra et al., 2014). One explanation is the loss of quality of radar-based Quantitative Precipitation Estimates (QPE) in mountainous regions: due to undesired ground echoes, partial or total beam blockage, the uncertainty due to the vertical variability of the radar reflectivity (e.g. Pellarin et al., 2002) and path attenuation caused by intense rainfall cells (the latter identified by Marra et al., 2014 as the dominant error for rainfall events triggering debris flows in Northeastern Italian Alps).

The goal of this work is threefold: i) the characterization of rainfall episodes in the Rebaixader catchment and the comparison of rainfall data that triggered torrential events and others that did not; ii) the definition of Intensity-Duration (ID) thresholds using rainfall data measured inside the catchment and applying two different techniques; and, iii) the discussion of some aspects related to the uncertainty on the definition of rainfall thresholds.

## **Rebaixader catchment (Central Pyrenees, Spain)**

## Morphology, geology and climate

The Rebaixader catchment is located in the upper Noguera Ribagorçana basin, in the South Central Pyrenees (Figure 1). The catchment faces the northwest and covers an area of 0.53 km<sup>2</sup>. The bedrock is formed by Devonian slates and phyllites. The catchment elevation ranges from 1345 m asl, at the fan apex, up to 2310 m asl at its highest point near the Planamorrans Peak of 2472 m asl. The initiation zone of the debris flows and debris floods is a steep (up to 70°) scarp formed in a lateral moraine. The material mainly consists of a sandy boulder. The thickness of the deposit usually exceeds 15 m; which suggests that the event size is not limited by availability of sediment. The source zone connects downslope with a 150 m long strongly incised channel. At the bottom of the catchment, the channel zone opens to a small fan, formed by the accumulation of the largest events.

The climate of the area is principally influenced by three factors: 1) the close distance to the Mediterranean Sea, 2) the effect of the west winds from the North Atlantic, and 3) the orographic control of the Pyrenean mountain range. The mean annual precipitation in the upper part of the Noguera Ribagorçana fluctuates between 800 mm and 1200 mm (Digital Climatic Atlas of Catalonia, 2004).

A preliminary analysis of the rainfall conditions triggering torrential events in the Rebaixader catchment showed that debris flows and debris floods are mainly caused by short and high-intensity rainstorms (Hürlimann et al., 2014). These rainstorms are associated with convective rainfall episodes that occur in the summer season. In addition, some minor torrential activity has also been observed in spring and autumn.

## Monitoring stations

In summer 2009, a monitoring network for debris flows and other torrential processes was installed in the Rebaixader catchment. Since then, the network has continuously been improved and includes at the moment six different recording stations (Figure 1).

Four stations are dedicated to sense the initiation mechanisms: two meteorological stations (“METEO” in Figure 1) and two infiltration stations (“INF”). The other two stations detect the passing of the torrential flows at several points (“FLOW”-station).

A total of eight geophones along the incised channel reach (see FLOW-stations in Figure 1) detect the torrential processes, when a selected threshold is exceeded (Abancó et al. 2014; Hürlimann et al. 2014). In addition, the flow depth is measured and a video camera takes a movie for visual interpretation of the passing flow.

The meteorological stations consist of standard tipping-bucket rain gauges and sensors recording the air temperature and the relative humidity of the air. The meteorological station that is used in this study is located next to the channel zone (METEO-CHA).

The two infiltration stations include soil moisture sensors and devices that register suction as well as soil temperature. Both stations are set up in the highest part of the initiation zone and on the top of the scarp (Figure 1).

Because of the remote location of the monitoring system, the power supply consists of solar panels and batteries and the data transmission is performed via GPRS communications.

*Figure 1 may be placed here*

## **Data sets**

We have analyzed three rainfall data sets: a) the measurements obtained by the rain gauge installed in the Rebaixader catchment (hereafter, referred to as “REBAIXADER dataset”); b) the data recorded by the gauges situated nearby the catchment; and, c) radar-based QPE.

The Rebaixader METEO-CHA station contains a RM YOUNG 52203 rain gauge with a resolution of 0.1 mm. The measurements have a sampling rate of 5 minutes and are recorded by a Campbell Scientific CR200 datalogger. In addition, other five rain gauges located nearby the Rebaixader catchment have been selected to analyze the spatial variability of the rainfall episodes. The locations and topographic values of all the rain gauges are given in Figure 1. The distances between the initiation area of the torrential flows in the Rebaixader torrent and the nearby gauges range from 3.6 to 16.4 km.

*Figure 2 may be placed here*

*Table 1 may be placed here*

Between July 2009 and October 2014, the total number of torrential flows detected in the Rebaixader catchment was 28. However, rainfall data are only available for 25 flows due to malfunctions of the meteorological station during three rainstorms. Finally, a total of 167 rainfall episodes were selected for the present analysis: 25 correspond to rainstorms that triggered torrential flows (from now on referred to as "TRIG"), while the remaining 142 did not trigger torrential flows (from now on referred to as "NonTRIG").

The definition of the rainfall duration is an important aspect for the analysis of triggering conditions and it can considerably influence the final outcomes, since the interpretation of the results are subject to the definition of the rainfall episode. The establishment of objective and clear criteria to define the duration of the rainfall episodes that cause landslides is object of many research studies (e.g. Berti et al., 2012, Melillo et al., 2014, Segoni et al., 2014b or Vessia et al., 2014). However it is a complex task, which has not yet been resolved. In this study, we fixed the duration by the condition that no precipitation was measured during one hour before and after the episode. This criterion is situated between the ones defined in other studies regarding rainfall triggers in monitored catchments: 6 hours without more than a trace (0.1 mm signal) at Illgraben

(Badoux et al., 2009) or at Moscardo (Deganutti et al. 2000); and a 10 minute gap before and after rainfall at Chalk Cliff (Coe et al., 2008).

Our selection of rainfall episodes (both TRIG and NonTRIG) is based on the fact that the daily rainfall was higher than 10 mm. However, it is possible that this daily rainfall (>10 mm) does not correspond to only single rainfall episode. In that case, more than one rainfall episode may be identified in one single day. The condition used to define the duration and derived parameters of rainfall episodes is that the no precipitation was observed one hour before and one hour after the rainfall.

The temporal distribution of the 167 selected rainfall episodes shows that most of the torrential flows occur in summer (Figure 3). The maximum is located in the month of July, when an average of 1.7 events has taken place during the 5 years of monitoring. At the same time, July is the month with the highest ratio of torrential flow occurrence over the total number of rainfall episodes: up to 70% of the rainfall episodes end in a torrential flow in July. Also, some events occurred in spring and autumn, while no event took place in winter. The triggering of spring torrential flows and rockfalls in the catchment is affected by snowmelt, which can influence the rainfall analysis due to the additional amount of water input (Hürlimann et al., 2010; Hürlimann et al. 2012). In this work, no distinction between seasonal behaviour has been applied, since there was not any possibility to distinguish between the melting snow and rainfall components of the generated runoff. However, in 2012, complementary instrumentation was installed in the site in order to quantify the effect of the snow melting on the triggering conditions of the torrential events and rockfalls.

*Figure 3 may be placed here*

## Methods

## Statistical analysis of rainfall data

The first step in the evaluation of the thresholds for the critical rainfalls at the Rebaixader consisted in the characterization of the rainfall episodes occurred at the catchment. A statistical analysis of the REBAIXADER dataset was performed to characterize the rainfall episodes in relation to the occurrence of torrential flows.

For such analysis, several parameters of the rainfall episodes were computed. The histograms of 18 parameters related to accumulated rainfall, duration of the rainfall episode, moving average of the rainfall intensities and antecedent rainfall calculated over several durations prior to the rainfall episode were plotted. After a first analysis of the distributions of the TRIG and NonTRIG datasets for the different parameters, a set of 10 variables was selected based on the most representative differences between the distributions of the two studied datasets.

Besides the analysis of the distributions, T-tests were performed using the statistical analysis software GraphPad Prism version 6.00 for Windows (GraphPad Prism, 2014) to determine if the differences between the TRIG and NonTRIG datasets were significant in statistical terms.

## Definition of rainfall thresholds

We defined thresholds by two different methods, using the variables that are more significantly different between TRIG and NonTRIG rainfalls. First, we calculated thresholds by plotting mean intensity ( $I$ ) and total duration ( $D$ ) of the rainfall events. This is the standard rainfall plotting method in landslide hazard analysis, in which each event is represented as a single point in a D-I plot. Second, we propose a new method to define thresholds based on the concepts of hydrology. In the following, both methods will be briefly summarized.

*Landslide method: Rainfall mean intensity – total duration*

Plots of mean intensity – total duration of rainfall events are the most common ones in landslide hazard assessment, because they can be used when high frequency measurements of the rainfall intensity (e.g. in 5-min intervals) are not available. This approach has been widely analyzed in many studies (e.g. Caine, 1980; Guzzetti et al., 2007, 2008) and can be expressed with a power-law model, which represents a correlation theoretically independent from any physical condition of the source area:

$$I = \alpha D^{-\beta} \quad (1)$$

where  $\alpha$  and  $\beta$  are the scale and shape parameters (the intercept and the slope of the power line in a log-log plot), which can be estimated by different fitting techniques. Herein, the thresholds defined with this method are abbreviated as  $T_{\text{tot}}$  and uses the total duration of the rainfall episode,  $D_{\text{tot}}$ .

In a first step, the line, which is defined by the best-fit power law through all the triggering rainfalls, was plotted. Then, parallel lines with the same slope  $\beta$  were drawn in order to define thresholds of different probability levels (70, 80, 90 95 and 100%). A similar technique was successfully applied by Brunetti et al. (2010) and Peruccaci et al. (2012) to minimize false positive alarms in a warning system. However triggering rainfalls that exceed the threshold lines were used herein to define the percentages. Finally, a simple ROC analysis was carried out to determine the most coherent percentile line using a representative sample of the data set.

*Hydrology method: Maximum floating intensity – floating duration*

In the following, we propose a new method to define thresholds based on the concepts of hydrology. The data of each rainfall episode are represented as multiple points in the I-D plot, each of them defined by a floating time interval with a minimum duration of 5 minutes (the scan rate of the Rebaixader METEO-CHA gauge). Following an approach frequently used in hydrology, the data of each rainfall episode are represented as

multiple points in a I-D plot, each of them defined as the maximum floating intensity for a number of different durations, with a minimum duration of 5 minutes (the scan rate of the Rebaixader METEO-CHA gauge). Therefore, the resulting ID curves are based on many points that represent the maximum rainfall intensity for specific time intervals. The thresholds established with this method use floating durations of the rainfalls,  $D_{fi}$ , and therefore, the resulting thresholds are abbreviated as  $T_{fi}$ . As in the previous method, thresholds with different probability levels were defined. However, the resulting thresholds in this second method were not straight lines, but curves passing through the different floating time interval,  $D_{fi}$ . These curves were calculated by the percentages of triggering rainfalls situated above the corresponding threshold. In order to better compare the two methods, straight lines were also determined for the threshold curves using the best-fit power law.

This second method provides additional information on the variability of the rainfall intensity during a rainfall episode. An advantage of this new method is the possibility of its straightforward implementation in an early warning system. In contrast, the variables used in the first method (the total duration and the mean rainfall intensity) can only be derived after the end of the rainfall episode.

## Results

### Statistical analysis of rainfall data

Figure 4 shows the histograms of ten different variables that describe the 167 selected rainfall episodes: 25 of them triggering torrential flows (TRIG) and 142 not triggering torrential flows (NonTRIG). These ten variables were selected from a larger group of variables and include the total rainfall amount, the duration of the rainfall episode and its intensity. In addition the rainfall of the previous one and three days was also

analyzed. In the histograms TRIG and NonTRIG rainfalls can be discerned, and frequency curves have been fitted to each of them. From a visual comparison, it can be observed that the frequency distribution for the duration (Figure 4b), antecedent 1-day rainfall (Figure 4f) and antecedent 3-day rainfall (Figure 4e) for TRIG rainfalls and NonTRIG rainfalls clearly overlap. The mode of the frequency curve for these variables is similar for both rainfall types. In contrast, the distributions of total rainfall, mean rainfall, maximum floating rainfall intensity for 1 hour, 5 minutes, 10 minutes, 30 minutes and 5 hours for TRIG and NonTRIG rainfall episodes show differences. For all these variables the frequency mode is higher in triggering rainfalls rather than in non-triggering rainfalls.

*Figure 4 may be placed here*

In order to prove the hypothesis that some of the variables show different patterns in TRIG and NonTRIG rainfall episodes, a t-test was carried out for all the analyzed variables. Here, the t-test was used to determine if the mean values of all the variables in Figure 4 are significantly different between TRIG and NonTRIG rainfall episodes.

The results of the t-test are shown in Figure 5. The P-value expresses the probability of observing a large difference between values from different groups, by asking whether the difference between the mean of two groups is likely to be due to chance. The null hypothesis (TRIG and NonTRIG rainfall episodes may show differences but only due to random sampling) is previously evaluated. The P-value is computed assuming that the null hypothesis is true, and takes high values if the null hypothesis is really true and low values if it is not true. In this work, the most common significance levels have been applied (0.1, 0.05, 0.01, 0.001 and 0.0001) in order to define several significance ranges between the levels established. In Figure 4, the results of the t-test are represented in box plots showing the median, maximum and minimum values and the quartiles. The rainfall variables that show the most significant difference between

groups are the intensity variables for short time intervals (Figure 5d, Figure 5g, Figure 5h and Figure 5j) and the total mean rainfall (Figure 5c). It can be easily observed that the values of the TRIG are higher than the NonTRIG rainfall episodes. In contrast, the variables of antecedent rainfall do not show significant differences between TRIG and NonTRIG rainfalls (Figure 4). For the duration (Figure 4), the difference between the two populations is also small, however it is significant. In this case, it can be observed that the duration of TRIG rainfalls is generally lower than the NonTRIG rainfalls.

*Figure 5 may be placed here*

### Rainfall thresholds

Figure 6 shows the typical plots of rainfall total duration ( $T_{tot}$ ) vs. mean intensity of episodes that triggered torrential flows and that did not trigger torrential flows. Figure 6 shows the threshold with higher performance found in the ROC analysis, which corresponds to the 90th percentile ( $T_{tot\_90\%}$ ) of the Intensity - Duration data points. The resulting threshold can be expressed as:

$$T_{tot\_90\%}: \quad I = 6.20 D^{-0.36} \quad (2)$$

*Figure 6 may be placed here*

Figure 7 shows the results obtained from the second method used for defining thresholds, in which the rainfall data of TRIG and NonTRIG were drawn by maximum floating intensities. For each rainfall episode, the curves have been extrapolated until 10 hours of duration, even if most of the rainfall episodes had shorter durations. In Figure 7a, the curves for all the analyzed rainfall episodes (TRIG and NonTRIG) are represented. For comparison, the intensity-duration curves corresponding to the return periods 10, 5, 2 and 1 year (data from the nearby rain gauge at Senet, which at the present is not working anymore) were added. This figure shows that only one of the TRIG rainfall episodes exceeds the 10 years return period. At the same time, most of

the TRIG rainfalls are below the 2 years return period line. This circumstance indicates that no exceptional rainfall is necessary in order to trigger a torrential flow event in the catchment, as it can be expected regarding the sub-annual frequency of these events in the Rebaixader catchment.

In Figure 7b, four percentile curves have been indicated, corresponding to 70%, 80%, 90% and 100% exceedance probabilities. As it was mentioned in the previous section, the lines of the percentiles were defined directly by calculating the corresponding percentage of TRIG rainfall episodes exceeding the threshold curves. The percentile 100% appears at a very low level, which can be explained due to a debris-flow triggered by a relatively small rainfall episode, occurred during spring, when most probably the effect of snowmelt has played an important factor. Again, the 90 percentile line was considered as the most representative one to approximate the triggering conditions. In this case, the several percentile lines were plotted to show the irregular shape of the lines (not straight lines like in the previous method). The following equations (3 – 7) show the best-fit power-law for the percentiles drawn in Figure 7b (Fig. 7b only shows the best fit of the 90% percentile points):

$$T_{fl\_70\%}: I = 8.71 D^{-0.71} \quad (3)$$

$$T_{fl\_80\%}: I = 7.86 D^{-0.70} \quad (4)$$

$$T_{fl\_90\%}: I = 5.49 D^{-0.75} \quad (5)$$

$$T_{fl\_95\%}: I = 4.26 D^{-0.75} \quad (6)$$

$$T_{fl\_100\%}: I = 3.42 D^{-0.73} \quad (7)$$

*Figure 7 may be placed here*

The 90% thresholds defined by the two methods for the Rebaixader torrent ( $T_{tot\_90\%}$  and  $T_{fl\_90\%}$ ) have different characteristics (Figure 8). The threshold derived from the floating intensities ( $T_{fl\_90\%}$ ) has a higher slope than the threshold of the total duration ( $T_{tot\_90\%}$ ). This difference indicates that the TRIG rainfall episodes have typically a higher intensity in short periods. In contrast, rainfalls with large total amounts but with small intensities require a larger duration in order to trigger a torrential flow at the Rebaixader catchment.

In Figure 6, it can be observed that 20% of the NonTRIG rainfalls exceed the  $T_{tot\_90\%}$ , while in Figure 7 only 5.6% of the NonTRIG rainfalls surpass the  $T_{fl\_90\%}$ . Table 2 shows the numbers and percentages of NonTRIG rainfalls that exceed the two different thresholds defined. Thus, they would have been identified as potentially TRIG rainfalls (false positives). Several cases have been considered: a) the number of NonTRIG rainfalls exceeding the  $T_{tot\_90\%}$  threshold, b) the number of NonTRIG rainfalls that totally exceed the  $T_{fl\_90\%}$  (which means that all of the points representing one rainfall are situated over the threshold), c) the number of NonTRIG rainfalls that exceed the  $T_{fl\_90\%}$  before 30 minutes of rainfall duration and d) the number of NonTRIG rainfalls that exceed  $T_{fl\_90\%}$  after 30 minutes of duration. Results indicate that more than 60% of the NonTRIG rainfalls would have exceeded the  $T_{fl\_90\%}$  at some point. However, half of the times the threshold would have been exceeded after 30 minutes of duration; and  $\frac{3}{4}$  of the times it would have been after 10 minutes. For the application of the threshold in a warning system this would be positive, since a false warning would have been issued only for 15% of the NonTRIG rainfalls.

The two thresholds can also be compared with other thresholds from the literature (Figure 8). On one side, thresholds defined for monitored catchments have been considered: three for debris-flow triggering, established at Moscardo (Deganutti et al., 2000), Illgraben (Badoux et al., 2009) and Chalk Cliffs (Coe et al., 2008), and two for sediment transport defined at Erlenbach (Badoux et al., 2012) and Rio Cordon (Badoux

et al., 2012). On the other side, we have also included two well-known thresholds defined at global scale were added (Caine 1980; Guzzetti et al., 2008). This comparison shows the similarity of our  $T_{fl\_90\%}$  threshold with the Illgraben threshold (rainfall until the trigger of the event), the Chalk Cliffs threshold, or the two thresholds for sediment transport. At the same time, the  $T_{tot\_90\%}$  shows a similar slope to the global thresholds, although the position in the plot is rather different.

*Figure 8 may be placed here*

The definition of the rainfall duration is a key point in the analysis of the rainfall thresholds for landslides and also for torrential flows. Since in most of the occasions the information of the initiation the torrential flow under consideration is not exactly known, the duration of the total rainfall (from the start of the rainfall until it finishes) is considered. However, it has been proved in the monitored Illgraben catchment (Switzerland) that considering the rainfall registered until the torrential flow occurs, may induce important changes in the definition of the rainfall thresholds (Badoux et al, 2012).

Three different criteria were used to define the rainfall event (Figure 9a): i) duration until the downslope moving torrential flow is detected by the monitoring station ( $D_{till\_trigger}$ ); ii) duration until the peak intensity of the rainfall ( $D_{till\_peak}$ ); and, iii) duration until the end of the rainfall ( $D_{total}$ ). The selection of the different durations has clear effects over both of the basic parameters for the definition of the rainfall thresholds: rainfall duration and rainfall intensity (Figure 9b and c). One should note the short duration of the rainfall, when the duration until the trigger of the torrential flow is considered. This fact may be explained due to a very short travel distance of the flows between the initiation zone and the detection point at the FLOW-station (Figure 1).

*Figure 9 may be placed here*

The three different criteria used for the definition of rainfall duration have been plotted in the total duration versus mean rainfall intensity plot (Figure 10). As for Figure 6, a 90%-threshold line has been determined for each criterion drawing a straight line parallel to the one that best fitted the rainfall points by a power law. As expected from the previous observation, the threshold for the duration until trigger is really low compared to the other two criteria. In contrast, the thresholds for the duration until the rainfall peak and for the total duration are slightly different, being the corresponding intensities of “till peak” threshold a bit higher than the ones for the criteria “total duration”. While the “total” threshold is the most successful in terms of predictability (maximum number of correctly predicted events), the “till trigger” threshold shows the highest imprecision.

*Figure 10 may be placed here*

## **Uncertainty due to the spatial variability of rainfall**

In this section, we have focused on the effect of the spatial variability of rainfall analyzing data from nearby gauges and as depicted from weather radar QPE; this analysis illustrates (i) how the spatial variability of the rainfall field can introduce additional uncertainty on the definition of the rainfall thresholds (as mentioned above, the use of thresholds derived from rainfall data measured away from the catchment typically underestimates the critical ID conditions), and (ii) the loss of representativeness of rain gauge observations located at different distances from the watershed.

Radar QPEs used here were produced with the Integrated Tool for Hydrometeorological Forecasting (EHIMI; Corral et al. 2009) from the volume scans of the Creu del Vent single-polarization Doppler C-band radar. The volume scans are used to produce 10-minute accumulation maps with a resolution of 1 km.

Three representative examples of torrential flows occurred at the Rebaixader catchment were selected to show how much the rainfall field spatially varied by comparing data from five different rain gauges and from the weather radar. The distance between the rain gauges and the initiation area of the torrential flows is indicated in Table 1. The data from the radar rainfall field was calculated for the pixel that covers the METEO-CHA rain gauge and the initiation area of the flows (white dot in Figure 11).

The selected events represent three different torrential flow processes: first, a debris flow (occurred in the 11<sup>th</sup> of July 2010), second, a debris flood (5<sup>th</sup> of August 2011), and third a debris flood (9<sup>th</sup> of October 2010). Figure 11 shows the spatial variability of the 30-minute radar rainfall accumulation of the debris flow event (11 July 2010 at 1400 UTC), corresponding to the period with highest rainfall intensities in the catchment. The figure illustrates how the strong variability of the rainfall field results in significant differences in the rainfall at the different rain gauges, as it is also evident from the hyetographs of Figure 12.

For the 2010 debris flow (Figure 12a), the radar data shows the best accordance with the data recorded inside the catchment (Rebaixader METEO-CHA). The Baserca rain gauge (3.6 km to the north in the same valley) experienced a delay of the rainstorm, but registered similar intensities. In contrast, the Barruera gauge (5.9km to the southeast, but in another valley) recorded almost no rainfall. For the 2011 debris flood (Figure 12b), the general conclusions are similar. The radar shows the best agreement with the rainfall records of the catchment. Most of the rain gauges show comparable

patterns in time, but reduced or even no intensities. As for the debris flow, Baserca recorded the most similar peak intensity to the one observed in the catchment, but again with a delay in time.

In conclusion, the analysis of three rainstorms that triggered torrential flows in the Rebaixader torrent showed that the spatial variability can be large. This fact can cause important errors while defining a threshold with data from a nearby raingauge. Thus, the closest raingauge must not always be the most representative and the understanding of the meteorological characteristics in a study area should be considered (Nikolopoulos et al, 2015).

*Figure 11 may be placed here*

*Figure 12 may be placed here*

In a second step, the rainfall records from rain gauges and radar QPE were compared with a rainfall threshold obtained in the previous section. The  $T_{tot\_90\%}$  threshold was selected, since high-frequency rainfall data from the surrounding rain gauges was not available (only 30-min recordings). The total duration vs. mean intensities plot was used to compare the different rainfall values with the threshold (Figure 13). According to the meaning of thresholds, a torrential flow should occur if a point representing the rainstorm exceeds the line. The results show that only the radar and the rain gauge METEO-CHA (inside the catchment) would have detected the three torrential flow events, while two other rain gauges would have detected only one. The 3 remaining rain gauges would have missed both events.

Although we only checked three events, the results show some evidences, how the use of data from different sources can affect not only the definition of the rainfall thresholds, but also their implementation in early warning systems. Similar conclusions have been obtained in recent studies on debris-flow triggering (e.g. Marra et al., 2014).

*Figure 13 may be placed here*

## Conclusions

The importance of rainfall thresholds for landslide triggering is widely proved, and so it is their relevance on hazard assessment analysis (Badoux et al., 2009; Berenguer et al., 2015; Jakob et al., 2006; Papa et al., 2013; Stähli et al., 2015; Tiranti and Rabuffetti, 2010). Their definition is a complex task, affected by large diverse uncertainties. Herein, three of them have been addressed and evaluated: i) the method to derive the thresholds, ii) the spatial variability of the rainfall field; and iii) the definition of the triggering rainfall.

The analysis of 25 rainfall episodes that triggered torrential flows at the Rebaixader catchment as well as 142 rainfall episodes that did not trigger torrential flows, all measured in a rain gauge is located inside the catchment, shows that torrential flows were triggered by short and intense rainstorms, most of them with a return period of less than 2 years. The torrential flows typically occur in summer, with a maximum in July, and more occasionally in spring. The initiation of these flows seems to be affected by snowmelt, which can influence the results obtained here due to the additional amount of water input. Thus, two different thresholds (one for spring and another for summer and autumn) should be defined in the future, when additional information will be gathered on this aspect.

The analysis of 167 rainfall episodes indicates that rainfall duration and antecedent rainfall do not show important differences between triggering and non-triggering rainfalls. In contrast, total rainfall, mean rainfall and maximum floating rainfall intensities are significantly different between triggering rainfalls and non-triggering rainfalls.

We found that using different criteria for defining the rainfall intensity and duration the threshold value which is obtained changes significantly. On one hand,  $T_{tot}$  – threshold obtained in the Rebaixader catchment is more similar to global thresholds, which were also derived using the mean rainfall intensity and total duration. On the other hand, the  $T_{fi}$  – threshold (which is based on maximum rainfall intensity for specific time intervals) fits rather well with those determined for monitored catchments.

Calculating  $T_{tot}$  and  $T_{fi}$  thresholds for different percentiles, the 90% percentile threshold were found to be more representative of the rainfall conditions triggering torrential flows in the Rebaixader catchment.

The hyetographs obtained from five nearby rain gauges and from weather radar for two rainstorms that triggered torrential flows at the Rebaixader show important differences among them. This latter finding supports the important effect of spatial variability for processes triggered by convective summer storms (e.g. Marra et al., 2014).

Comparing the  $T_{tot_{90\%}}$  - thresholds established from measurement inside the catchment and from the nearby rain gauges and weather radar data revealed: first, that a nearby rain gauge located outside of the catchment under consideration is not always giving the best results, especially if the gauge is positioned in a neighboring valley; and second, that radar measurements strongly improve the results. Unfortunately, radar data are not available everywhere and the estimation of precipitation require more time.

Finally, criterion used to define the duration of a triggering rainfall also influences in the value of the threshold that is obtained. The thresholds calculated for the duration until peak and the total duration are similar. In contrast, the threshold for the duration until trigger is lower. This is probably a consequence of the small size of the Rebaixader catchment, which leads to a short reaction time between rainfall onset and the initiation of the torrential flows.

Although many uncertainties are still remaining and: a) additional data must be gathered and analyzed and b) uncertainties should be quantified, the outcomes of this research improve the knowledge on the definition of critical rainfall patterns for torrential flows. Since rainfall thresholds are the base of most warning systems for torrential flows and other types of rainfall-induced landslides, the results of this study also helps researchers and practitioners that are working on this subject in order to better inform on the probability of future events.

## **Acknowledgements**

We acknowledge the Catalan Weather Service (SMC) for providing the radar data and SMC and the Catalan Water Agency for providing rain gauge observations.

This research has been funded by the Spanish Ministry MINECO contract CGL2011-23300 (project DEBRISTART). The authors acknowledge the constructive comments of the F. Marra, an anonymous reviewer and the guest editor I. Braud.

## References

Abancó C., Hürlimann, M., Sempere, D. Berenguer, M., 2012. Benefits and limitations of using the weather radar for the definition of rainfall thresholds for debris flows. Case study from Catalonia (Spain). *Geophysical Research Abstracts*. Vol. 14, EGU2012-2683.

Abancó, C., Hürlimann, M., Moya, J., 2014. Analysis of the ground vibration produced by debris flows and other torrential processes at the Rebaixader monitoring site (Catalan Pyrenees, Spain). *Natural Hazards and Earth System Science*. 14, 929-943.

Badoux, A., Graf, C., Rhyner, J., Kuntner, R., McArdell, B., 2009. A debris-flow alarm system for the Alpine Illgraben catchment: design and performance. *Nat. Hazards* 517–539.

Badoux, A., Turowski, J.M., Mao, L., Mathys, N., Rickenmann, D., 2012. Rainfall intensity–duration thresholds for bedload transport initiation in small Alpine watersheds. *Nat. Hazards Earth Syst. Sci.* 12, 3091–3108.

Berenguer, M., Sempere-Torres, D., Hürlimann, M., 2015. Debris-flow forecasting at regional scale by combining susceptibility mapping and radar rainfall. *Nat. Hazards Earth Syst. Sci.* 15, 587–602.

Berti M, Martina MLV, Franceschini S, Pignone S, Simoni A, Pizziolo M., 2012. Probabilistic rainfall thresholds for landslide occurrence using a Bayesian approach. *J Geophys Res* 117:F04006.

Borga, M., Stoffel, M., Marchi, L., Marra, F., Jakob, M., 2014. Hydrogeomorphic response to extreme rainfall in headwater systems: Flash floods and debris flows. *J. Hydrol.* 518, Part , 194–205.

Brunetti, M.T., Peruccacci, S., Rossi, M., Luciani, S., Valigi, D., Guzzetti, F., 2010. Rainfall thresholds for the possible occurrence of landslides in Italy. *Nat. Hazards Earth Syst. Sci.* 10, 447–458.

Caine, N., 1980. The rainfall intensity-duration control of shallow landslides and debris flows. *Geogr. Ann.* 62A, 23–27.

Cepeda, J., Höeg, K., Nadim, F., 2010. Landslide-triggering rainfall thresholds: A conceptual framework. *Q. J. Eng. Geol. Hydrogeol.* 43, 69–84.

Coe, J.A., Kinner, D.A., Godt, J.W., 2008. Initiation conditions for debris flows generated by runoff at Chalk Cliffs, central Colorado. *Geomorphology* 96, 270–297.

Corral, C., D. Velasco, D. Forcadell, and D. Sempere-Torres, 2009. Advances in radar-based flood warning systems. The EHIMI system and the experience in the Besòs flash-flood pilot basin, in: *Flood Risk Management: Research and Practice*, edited by P. Samuels, S. Huntington, W. Allsop and J. Harrop, pp. 1295-1303, Taylor & Francis, London, UK, 1295-1303.

Crosta, G.B., Cucchiaro, S., Frattini, P., 2003. Validation of semi-empirical relationships for the definition of debris-flow behavior in granular materials, in: Rickenmann, D., Chen, C. (Eds.), *3rd Int. Conf. on Debris-Flow Hazards Mitigation*. Millpress, Davos, pp. 821–831.

Crozier, M. J., and Glade, T.: Frequency and magnitude of landsliding: fundamental research issues., *Zeitschrift fu'r Geomorphologie*, 115, 141-155, 1999

Cui, P., Chen, X., Waqng, Y., Hu, K., Li, Y., 2005. Jiangjia Ravine debris flows in southwestern China, in: Jakob, M., Hungr, O. (Eds.), *Debris-Flow Hazards and Related Phenomena*. Springer, Berlin, pp. 565–594.

De Vita, P., Reichenbach, P., Bathurst, J.C., Borga, M., Crosta, G., Crozier, M.J., Glade, T., Guzzetti, F., Hansen, A., Wasowski, J., 1998. Rainfall-triggered landslides: a reference list. *Environ. Geol.* 35, 219–233.

Deganutti, A.M., Marchi, L., Arattano, M., 2000. Rainfall and debris-flow occurrence in the Moscardo basin (Italian Alps), in: Wieczorek, G.F., Naeser, N.D. (Eds.), 2nd International Conference on Debris-Flow Hazards Mitigation. Balkema, pp. 67–72.

Digital Climatic Atlas of Catalonia, 2004. <http://www.opengis.uab.cat/acdc/> Last accessed 22 May 2015

Godt, J.W., Baum, R.L., Savage, W.Z., Salciarini, D., Schulz, W.H., Harp, E.L., 2008. Transient deterministic shallow landslide modeling: Requirements for susceptibility and hazard assessments in a GIS framework. *Eng. Geol.* 102, 214–226.

GraphPad Prism User Guide, 2014.

Guzzetti, F., Peruccacci, S., Rossi, M., Stark, C.P., 2008. The rainfall intensity-duration control of shallow landslides and debris flows: an update. *Landslides* 5, 3–17.

Guzzetti, F., Peruccacci, S., Rossi, M., Stark, C.P., 2007. Rainfall thresholds for the initiation of landslides in central and southern Europe. *Meteorol. Atmos. Phys.* 98, 239–267.

Hungr, O., Leroueil, S., Picarelli, L., 2014. The Varnes classification of landslide types, an update. *Landslides* 11, 167–194.

Hürlimann, M., Abancó C., Moya, J. 2010. Debris-flow initiation affected by snowmelt. Case study from the Senet monitoring site, Eastern Pyrenees. Proceedings of the "Mountain Risks: Bringing science to society" International Conference. Firenze, Italy, p.81-86.

Hürlimann, M., Abancó, C., Moya, J., 2012. Rockfalls detached from a lateral moraine during spring season. 2010 and 2011 events observed at the Rebaixader debris-flow monitoring site (Central Pyrenees, Spain). *Landslides*, 3, 385-393.

Hürlimann, M., Abancó, C., Moya, J. and Vilajosana, I., 2014. Results and experiences gathered at the Rebaixader debris-flow monitoring site, Central Pyrenees, Spain, *Landslides*.11(6), 939-953.

Jakob, M., Holm, K., Lange, O., Schwab, J.W., 2006. Hydrometeorological thresholds for landslide initiation and forest operation shutdowns on the north coast of British Columbia. *Landslides* 3, 228–238.

Jakob, M., Hungr, O., 2005. *Debris-flow Hazards and Related Phenomena*. Springer, Berlin.

Jakob, M., Owen, T., Simpson, T., 2012. A regional real-time debris-flow warning system for the District of North Vancouver, Canada. *Landslides* 9, 165–178.

Jibson, R.W., 1989. Debris flows in southern Puerto Rico. *Geol. Soc. Am. Spec. Pap.* 236, 29–56.

Katzensteiner, H., Bell, R., Petschko, H., and Glade, T.: The relationship between extreme precipitation events and landslides distribution in 2009 in Lower Austria, *Geophysical Research Abstracts*, 14, 2012.

Marchi, L., Cavalli, M., Sangati, M., Borga, M., 2009. Hydrometeorological controls and erosive response of an extreme alpine debris flow. *Hydrol. Process.* 23, 2714–2727.

Marra, F., Nikolopoulos, E.I., Creutin, J.D., Borga, M., 2014. Radar rainfall estimation for the identification of debris-flow occurrence thresholds. *J. Hydrol.* 519, Part , 1607–1619.

Melillo, M., Brunetti, M. T., Perucacci, S., Gariano, S. TL., Guzzetti, F., 2014. An algorithm for the objective reconstruction of rainfall events responsible for landslides. *Landslides*, pp.2399-2408.

Nikolopoulos, E.I., Crema, S., Marchi, L., Marra, F., Guzzetti, F., Borga, M., 2014. Impact of uncertainty in rainfall estimation on the identification of rainfall thresholds for debris flow occurrence. *Geomorphology* 221, 286–297.

Nikolopoulos, E.I., M. Borga, J.D. Creutin and F. Marra 2015: Estimation of debris flow triggering rainfall: influence of rain gauge density and interpolation methods. *Geomorphology*, 243 (2015), 40-50.

Papa, M.N., Medina, V., Ciervo, F., Bateman, A., 2013. Derivation of critical rainfall thresholds for shallow landslides as a tool for debris flow early warning systems. *Hydrol. Earth Syst. Sci.* 17, 4095–4107.

Pellarin, T., G. Delrieu, G. M. Saulnier, H. Andrieu, B. Vignal, and J. D. Creutin, 2002: Hydrologic visibility of weather radar systems operating in mountainous regions: Case study for the Ardeche Catchment (France). *Journal of Hydrometeorology*, 3, 539-555.

Peruccacci, S., Brunetti, M. T., Luciani, S., Vennari, C., and Guzzetti, F.: Lithological and seasonal control of rainfall thresholds for the possible initiation of landslides in central Italy, *Geomorphology*, 139–140, 79–90, 2012.

Restrepo, P., Jorgensen, D. P., Cannon, S. H., Costa, J., Laber, J., Major, J., Martner, B., Purpura, J., and Werner, K.: Joint NOAA/NWS/USGS Prototype Debris Flow Warning System for Recently Burned Areas in Southern California. *Bull. American Meteorological Society*, 89, 1845-1851.

Segoni, S., Rosi, A., Rossi, G., Catani, F., and Casagli, N. 2014a: Analysing the relationship between rainfalls and landslides to define a mosaic of triggering thresholds for regional-scale warning systems, *Nat. Hazards Earth Syst. Sci.*, 14, 2637-2648

Segoni, S., Rossi, G., Rosi, A., and Catani, F, 2014b.: Landslides triggered by rainfall: a semiautomated procedure to define consistent intensity-duration thresholds, *Comput. Geosci.*, 3063, 123-131

Stähli, M., Sättele, M., Huggel, C., McArdell, B.W., Lehmann, P., Van Herwijnen, A., Berne, A., Schleiss, M., Ferrari, A., Kos, A., Or, D., Springman, S.M., 2015. Monitoring and prediction in early warning systems for rapid mass movements. *Nat. Hazards Earth Syst. Sci.* 15, 905–917.

Tiranti, D., Rabuffetti, D., 2010. Estimation of rainfall thresholds triggering shallow landslides for an operational warning system implementation. *Landslides* 7, 471–481.

Vessia, G., Parise, M., Brunetti, M. T., Peruccacci, S., Rossi, M., Vennari, C., Guzzetti, F., 2014. Automated reconstruction of rainfall events responsible for shallow landslides. *Nat. Hazards Earth Syst. Sci.*, 14, pp. 2399-2408

Wieczorek, G.F., Glade, T., 2005. Climatic factors influencing occurrence of debris flow, in: Jakob, M., Hungr, O. (Eds.), *Debris-Flow Hazards and Related Phenomena*. Springer, Berlin, pp. 325–362.

Wilson, R.C., Wieczorek, G.F., 1995. Rainfall thresholds for the initiation of debris flows at La Honda, California. *Environ. Eng. Geosci.* 1, 11–27.

#### List of Tables:

Table 1: Topographic values of the rain gauges incorporated in this study.

Name of weather station	Altitude (m asl)	Distance to initiation area (km)
Rebaixader METEO-CHA	1365	0.4
Barruera	1090	5.9

Baserca	1450	3.6
Boí	2535	13.7
Lac Redon	2247	10.5
Pont de Suert	823	16.4

Table 2: Summary of false positives (NonTRIG rainfalls over the thresholds) according different criteria (see text for explanation on criteria definition).

	# of false positives	% of false positives over NonTRIG rainfalls
Exceeding $T_{tot\_90\%}$	29	20.4%
Complete exceeding $T_{fl\_90\%}$	8	5.6%
Exceeding $T_{fl\_90\%}$ in $\leq 10$ min	22	15.49%
Exceeding $T_{fl\_90\%}$ in $\leq 30$ min	43	30.2%
Exceeding $T_{fl\_90\%}$ in $> 30$ min	51	35.9%

**List of Figures:**

Figure 1: The Rebaixader catchment. Ortophoto of the catchment and the situation of the monitoring stations (rectangles: METEO stands for meteorological station, FLOW for flow dynamics station and INF for infiltration station). The dot shows the position of the raingauge METEO-CHA used in this study. The dashed white line indicates the drainage basin and the solid white line the fan. The inset illustrates the location of the Rebaixader catchment and the Creu Del Vent C-band weather radar, located in the municipality of La Panadella.

Figure 2: Location of the rain gauges analyzed in this study.

Figure 3: Monthly occurrence of TRIG rainfall events and NonTRIG rainfall events analysed in this study. The average monthly rainfall at the catchment is also indicated (Digital Climatic Atlas of Catalonia, 2004).

Figure 4: Histograms showing some rainfall characteristics (a: total rainfall, b: duration, c: mean rainfall, d: maximum floating 1-hour rainfall intensity, e: antecedent 3-day rainfall, f: antecedent 1-day rainfall, g: maximum floating 5-minutes rainfall intensity, h: maximum floating 10-minutes rainfall intensity, i: maximum floating 30-minutes rainfall intensity, j: maximum floating 5-hours rainfall intensity) of 167 rainfall episodes occurred at the Rebaixader catchment between July 2009 and October 2014. Rainfall episodes that triggered torrential flows (TRIG) and that did not (NonTRIG) are discerned. Normal distributions have been fitted to all the histograms.

Figure 5: Box plots for most of the variables in Figure 4. TRIG and NonTRIG are discerned, and the results of t-test are represented. The median is represented by the line inside the box, and the first and third quartiles are the extremes of the box, the maximum and minimum values are indicated by the end of the lines at the extremes of the box. See Table 1 for the abbreviation of the rainfall variables.

Figure 6: Mean intensity versus total duration relationship of rainfalls triggering torrential flows (TRIG) and rainfall not triggering torrential flows (NonTRIG). The 90% threshold is also indicated (see text for explanations how this threshold is established).

Figure 7: Maximum floating intensity versus duration relationship of rainfalls triggering torrential flows (TRIG) and rainfalls not triggering torrential flows (NonTRIG). a) Comparison between rainfall data observed at Rebaixader and rainfall return periods calculated for the nearby raingauge at Senet. b) Thresholds corresponding to different percentiles plotted as dotted edged lines and the final 90% threshold as straight best-fit line.

Figure 8: Selected threshold of the Rebaixader catchment versus other existing thresholds.

Figure 9: Effect of the definition of different duration. a) Graph illustrating the three types of durations. Histograms of duration (b) and on the mean rainfall intensity (c) for the 25 rainfalls triggering torrential flows in Rebaixader.

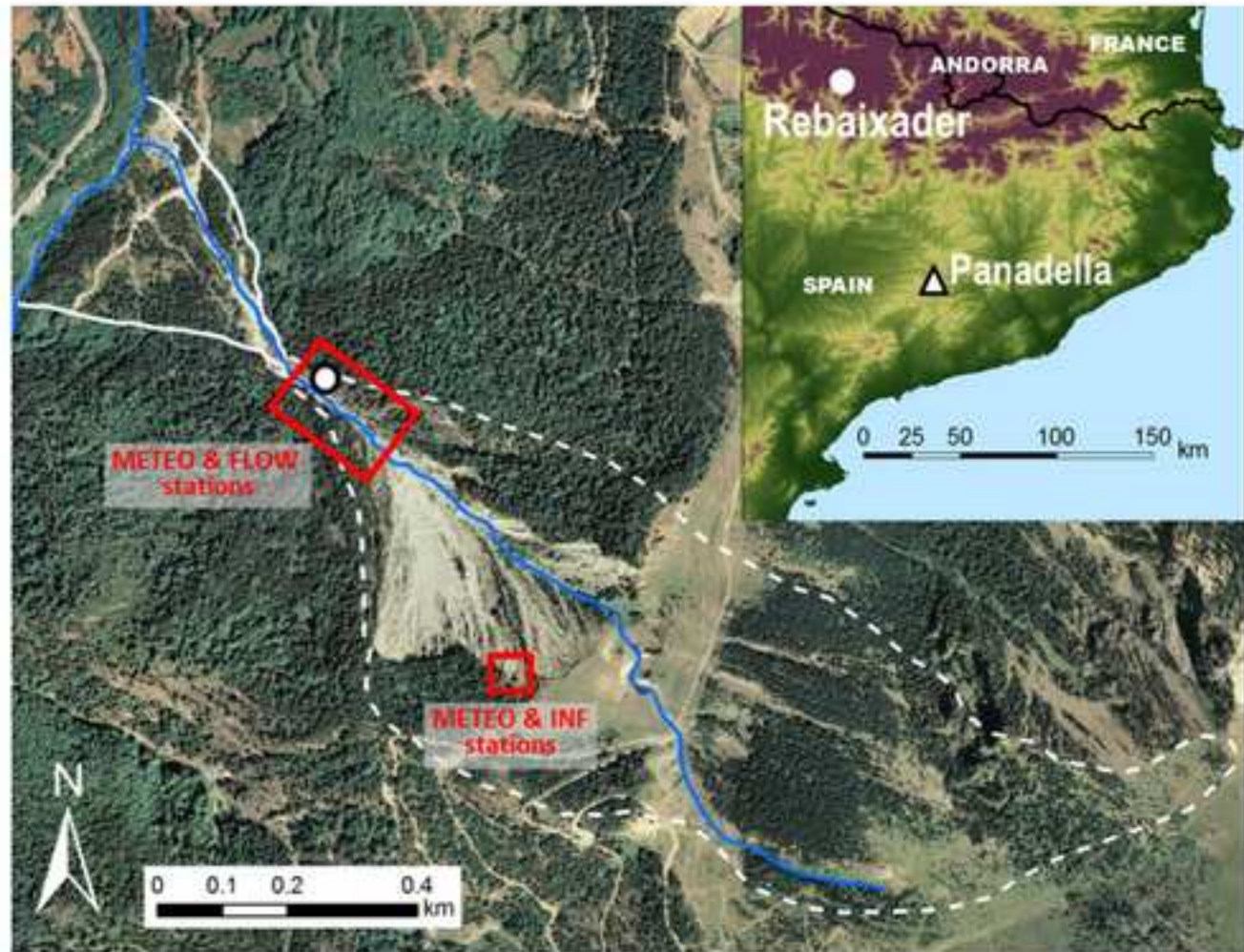
Figure 9: Duration versus mean rainfall intensity of the 25 rainfall episodes triggering torrential flows in Rebaixader distinguishing between the three types of durations. The 90%-thresholds of each dataset are also illustrated.

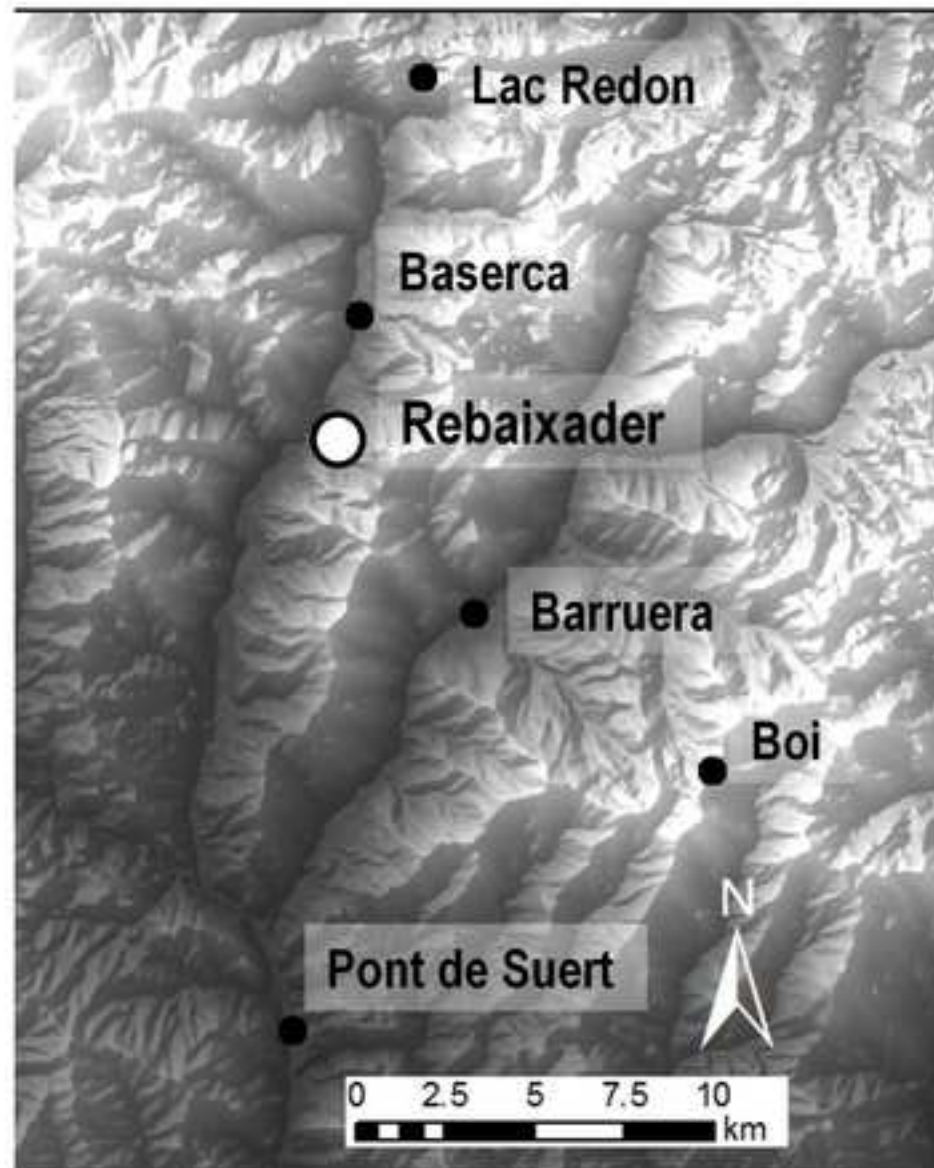
Figure 11: Radar measurements of the rainfall that triggered a debris flow in the Rebaixader torrent (white dot) on July 11th 2010. Data are represented as accumulated rainfall, Pacc, between 13:30 and 14:00. Black dots indicate the meteorological stations used.

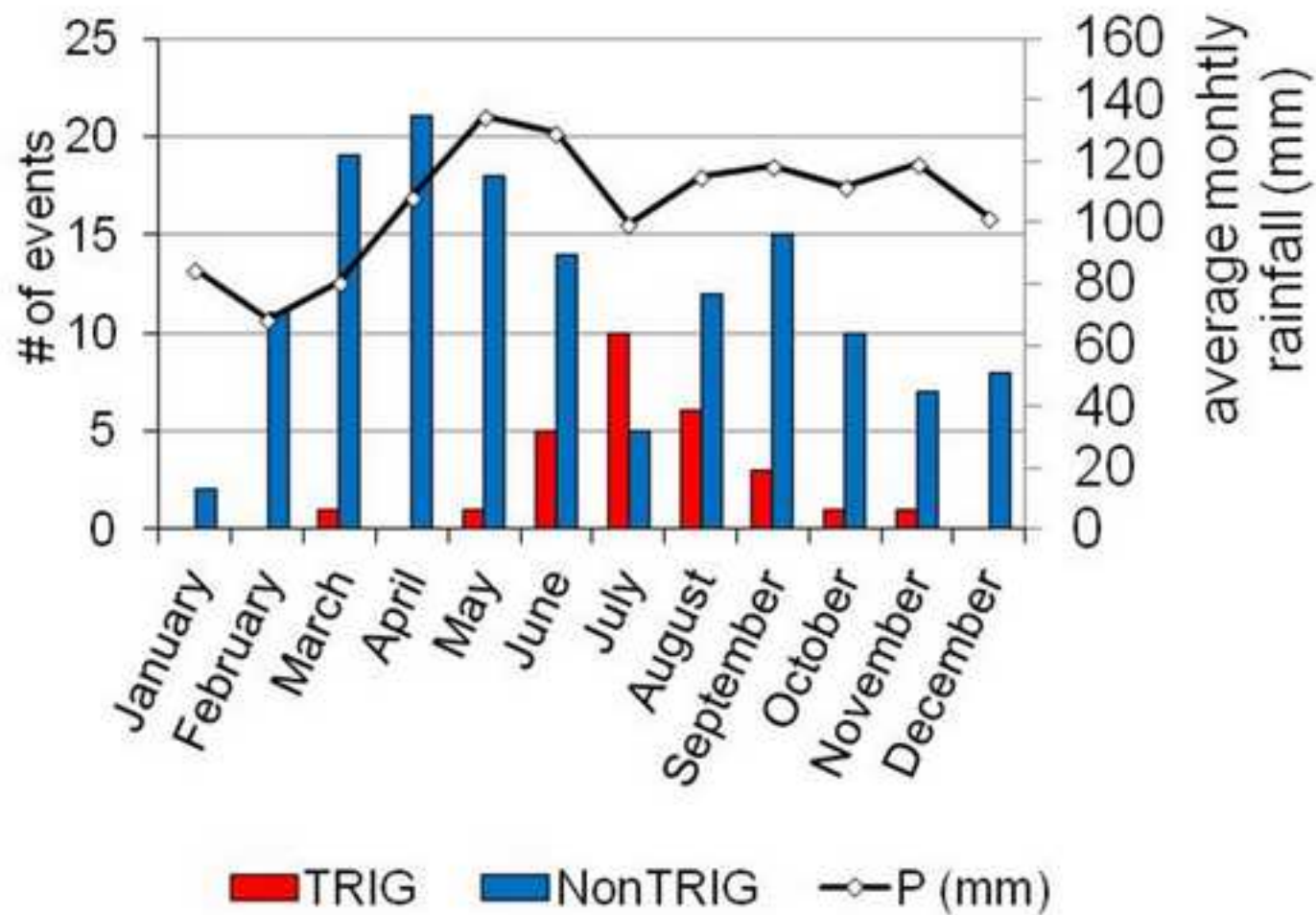
Figure 10: Comparison of the hyetographs obtained by raingauges and Doppler radar concerning the debris flow on July 11<sup>th</sup> 2010 (a), the debris flood on August 5<sup>th</sup> 2011 (b) and the debris flood on October 9<sup>th</sup> 2010. Radar measurements are shown for the scarp, which is the initiation area.

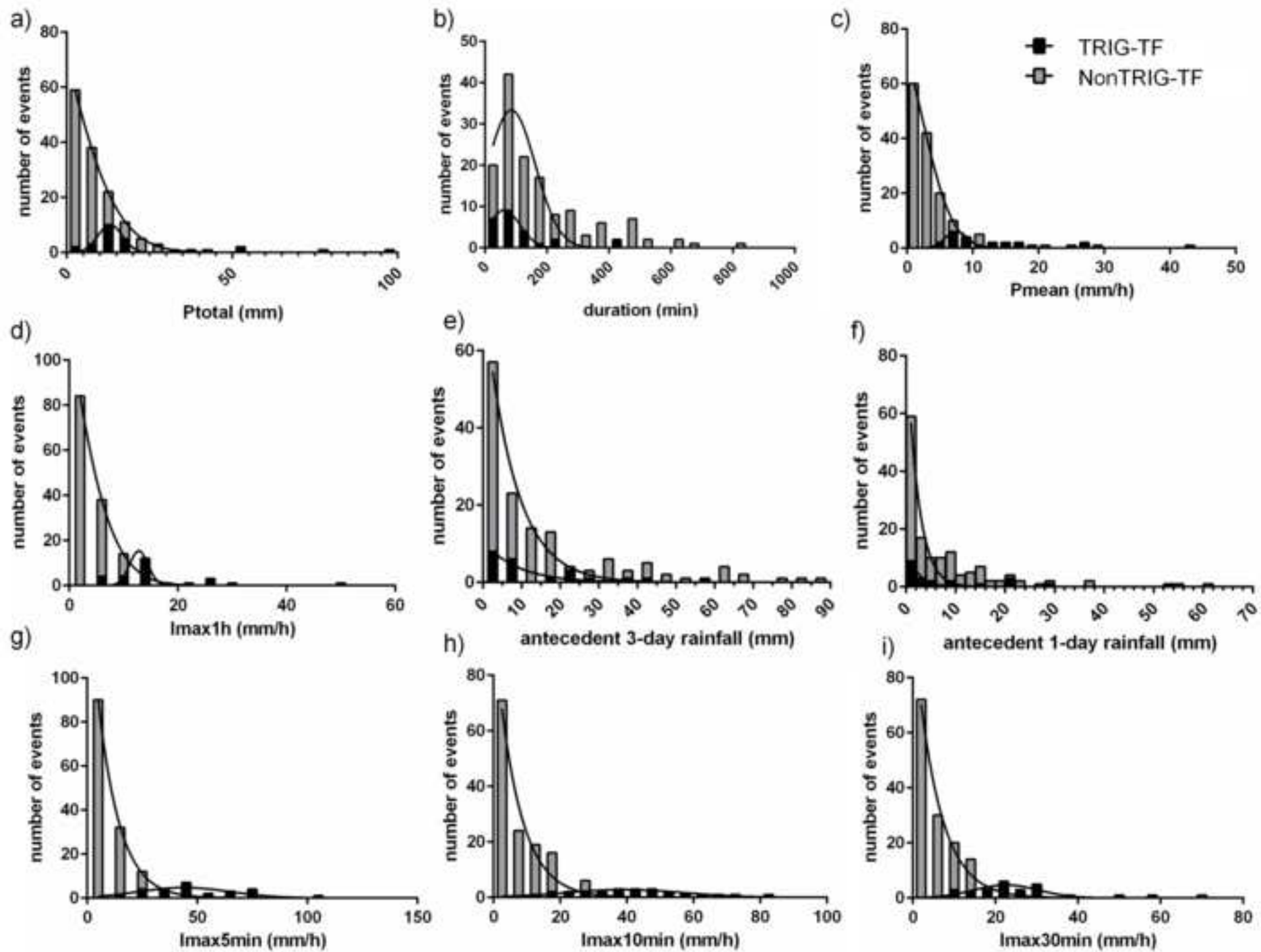
Figure 11: Total duration-mean intensity values for the three selected torrential flows (debris flow July 11, 2010 and debris floods October 9, 2010 and August 5, 2011) obtained by raingauges and Doppler radar. The 90%-threshold of the “total duration method” is illustrated for comparison.

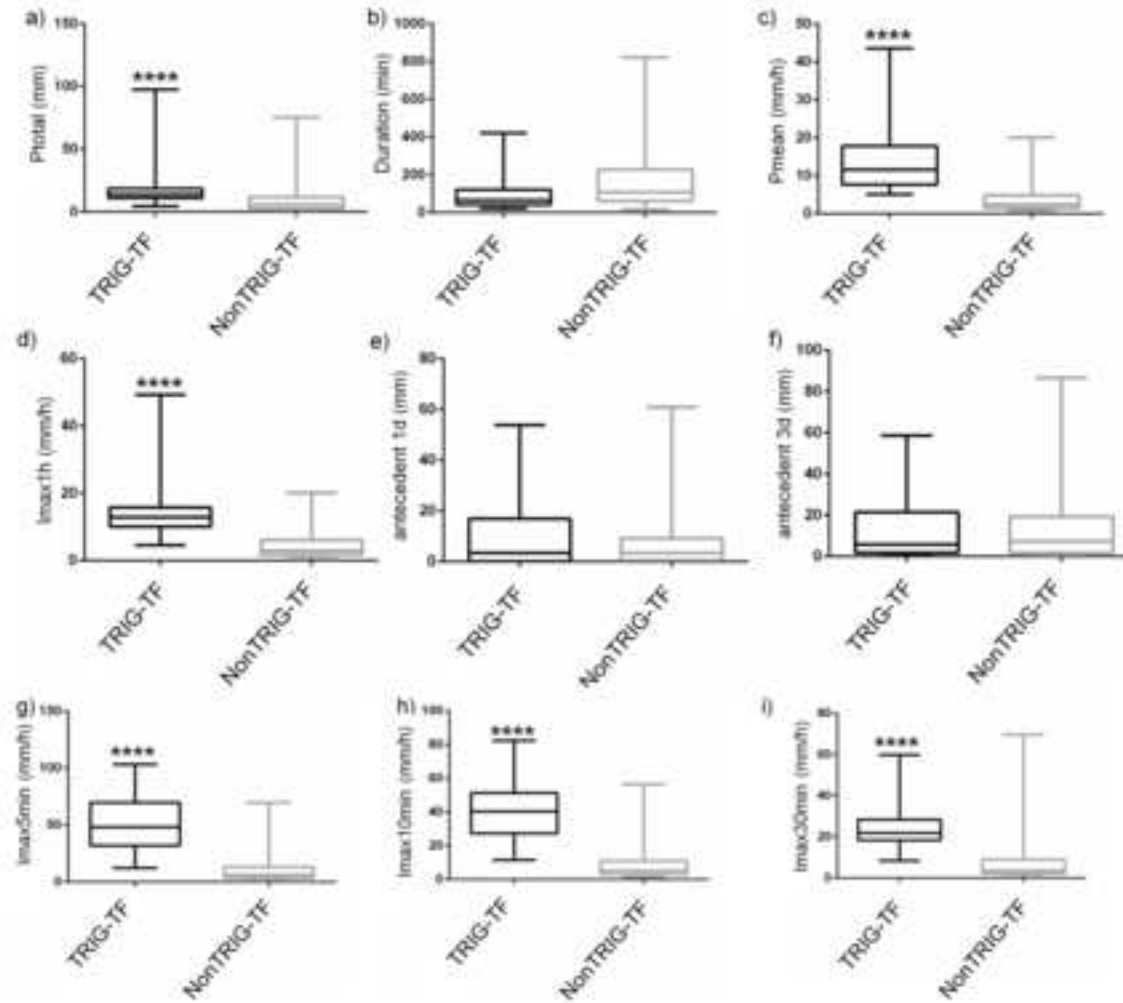
ACCEPTED MANUSCRIPT





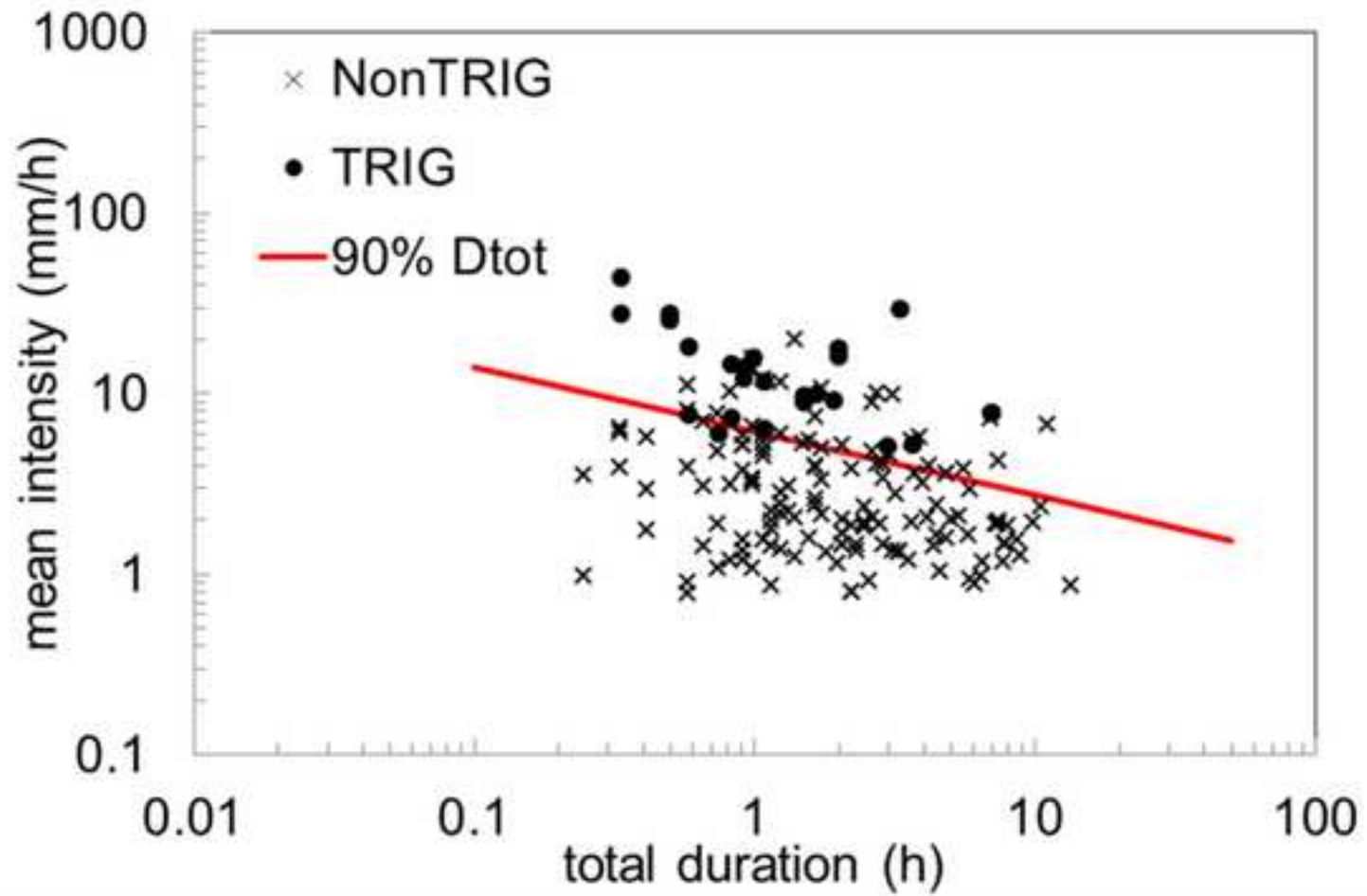


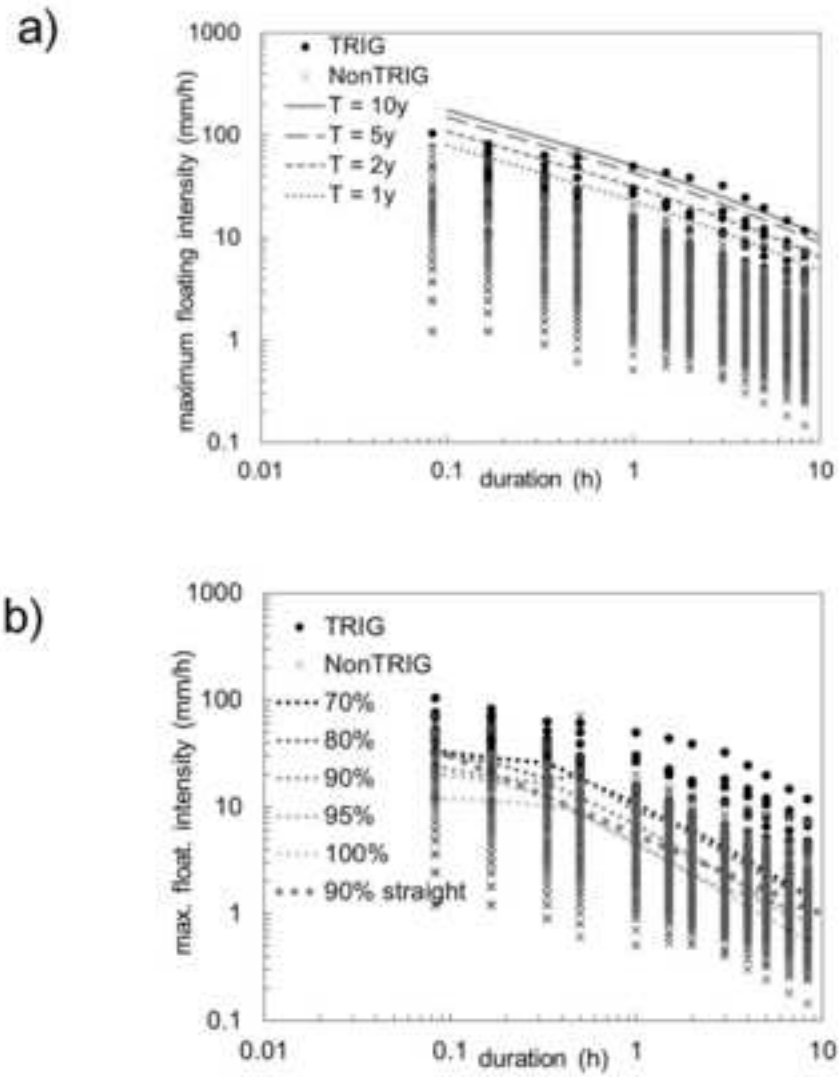


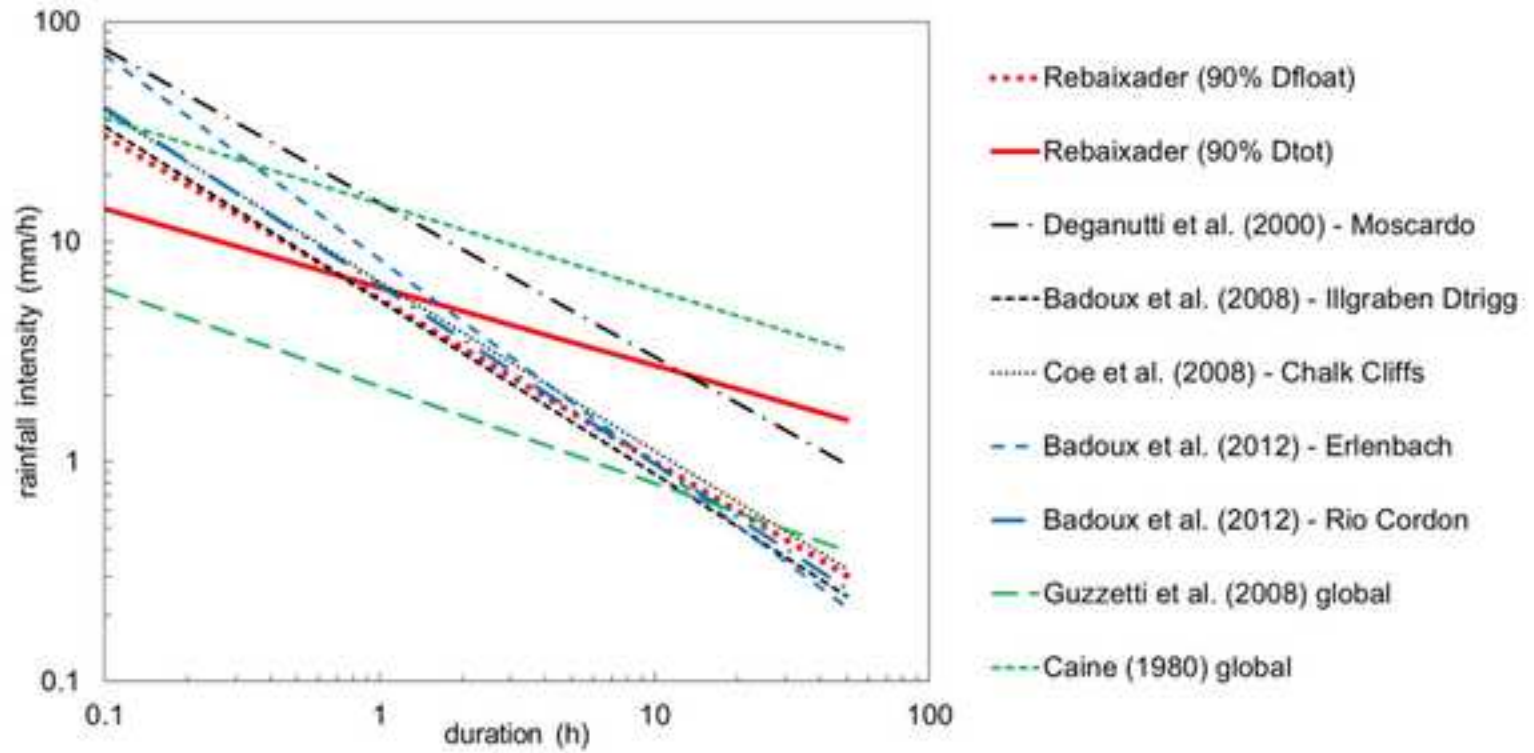


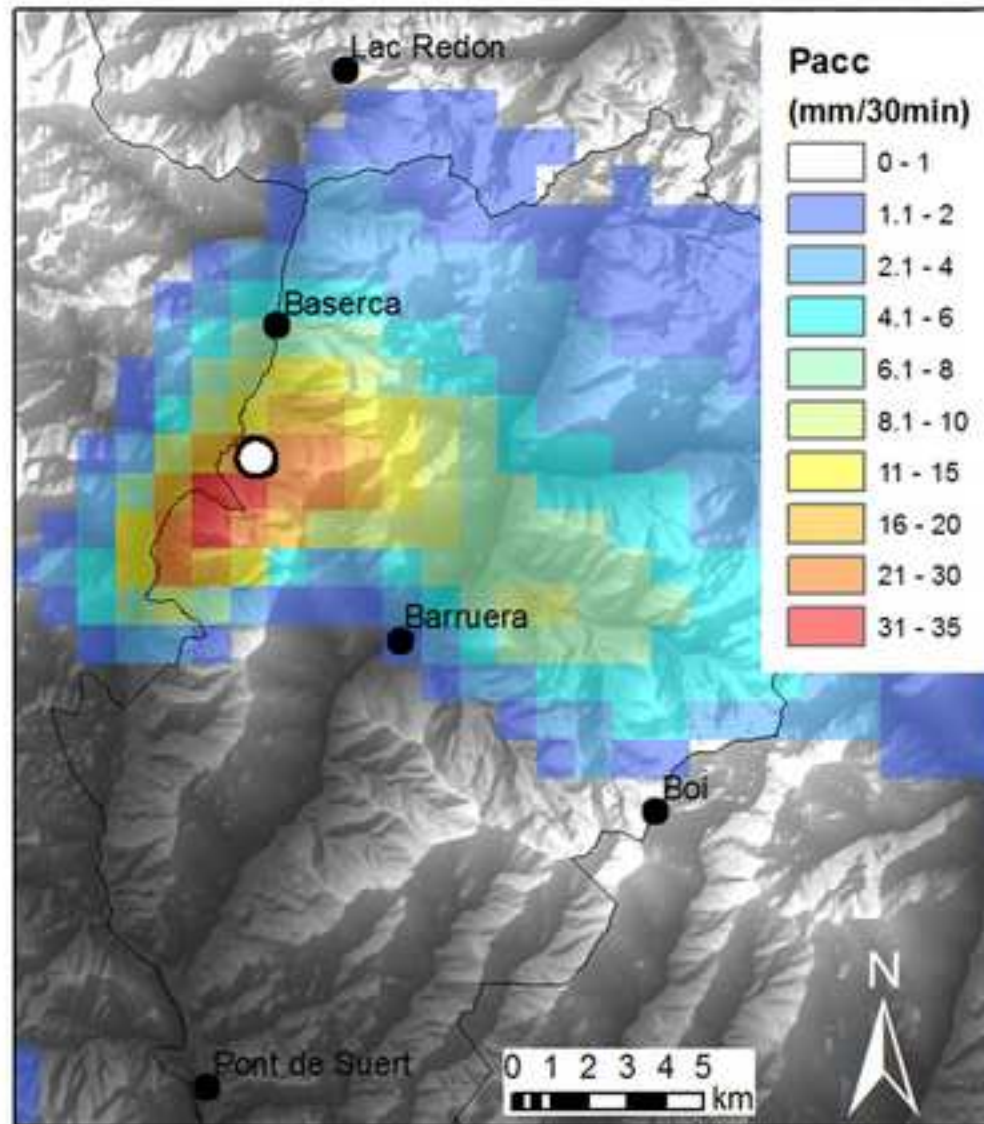
## T-test significance level

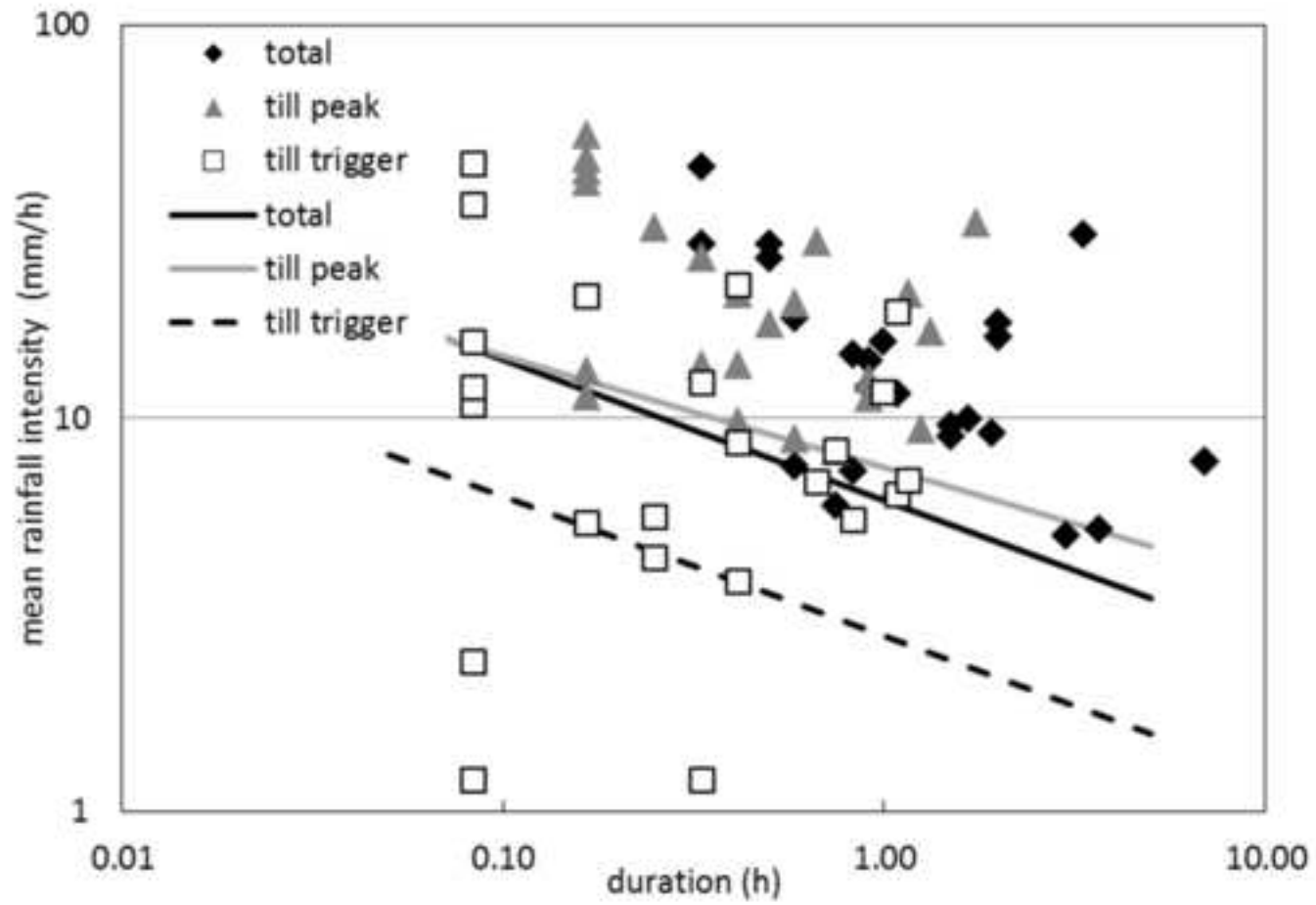
- $P > 0.05$  → Not significantly different
- \* →  $0.01 < P < 0.05$
- \*\* →  $0.001 < P < 0.01$
- \*\*\* →  $0.0001 < P < 0.001$
- \*\*\*\* →  $P < 0.0001$  → Difference highly significant

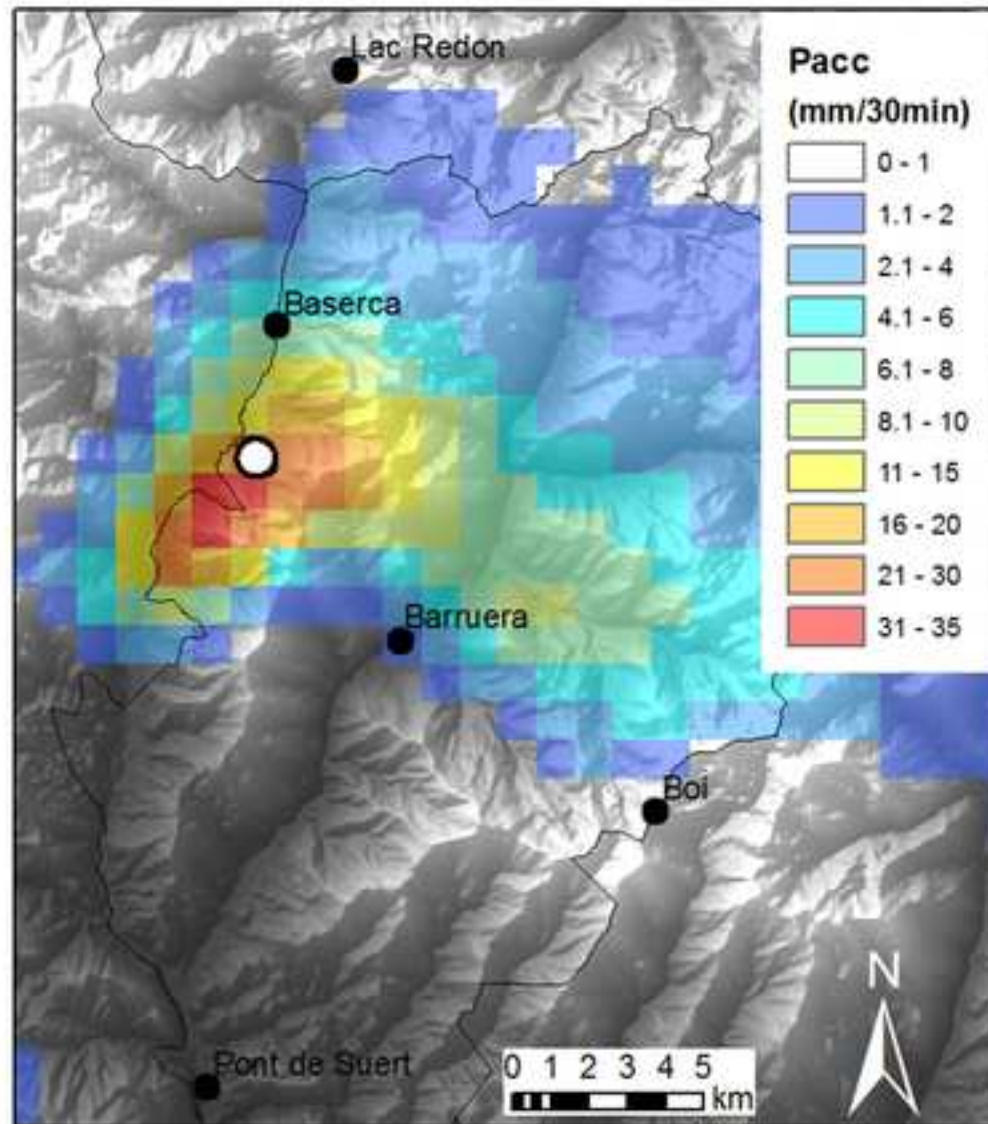


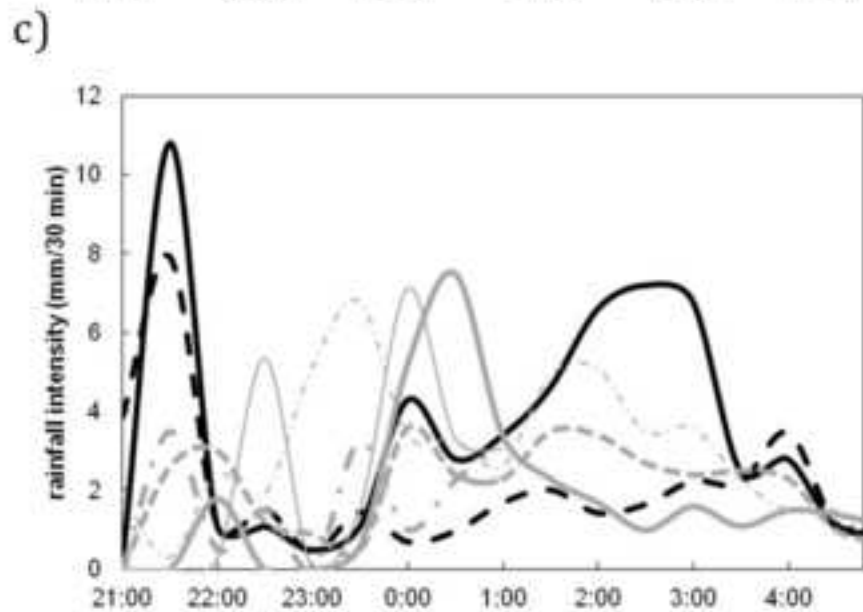
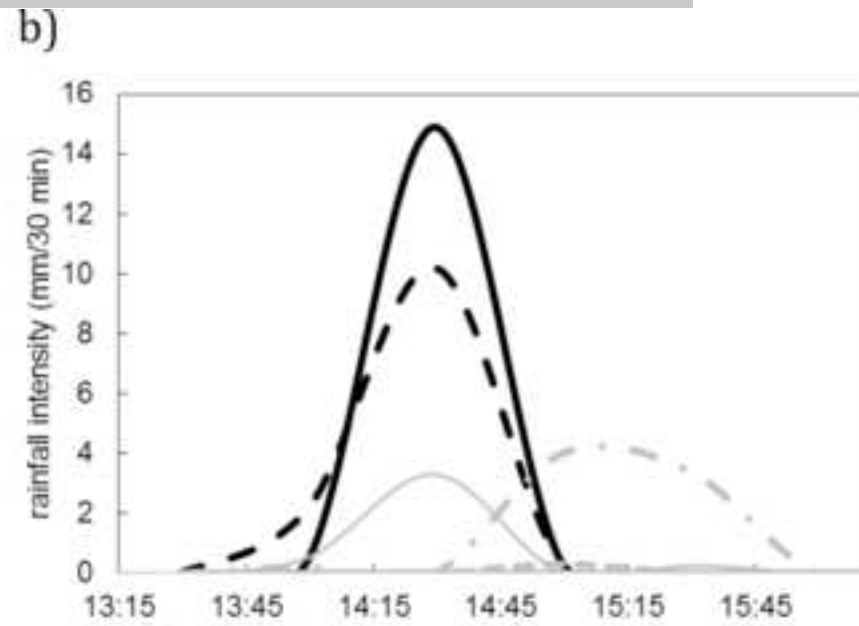
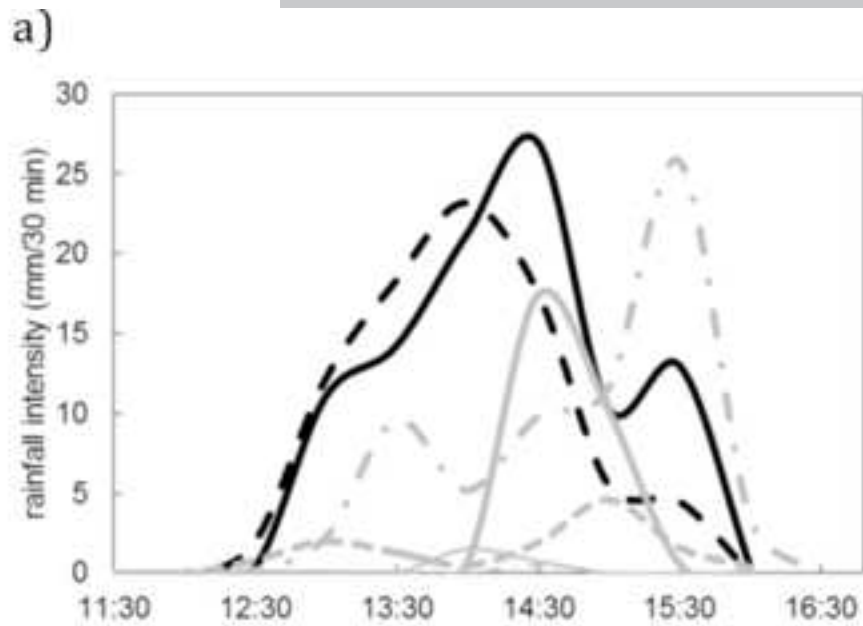


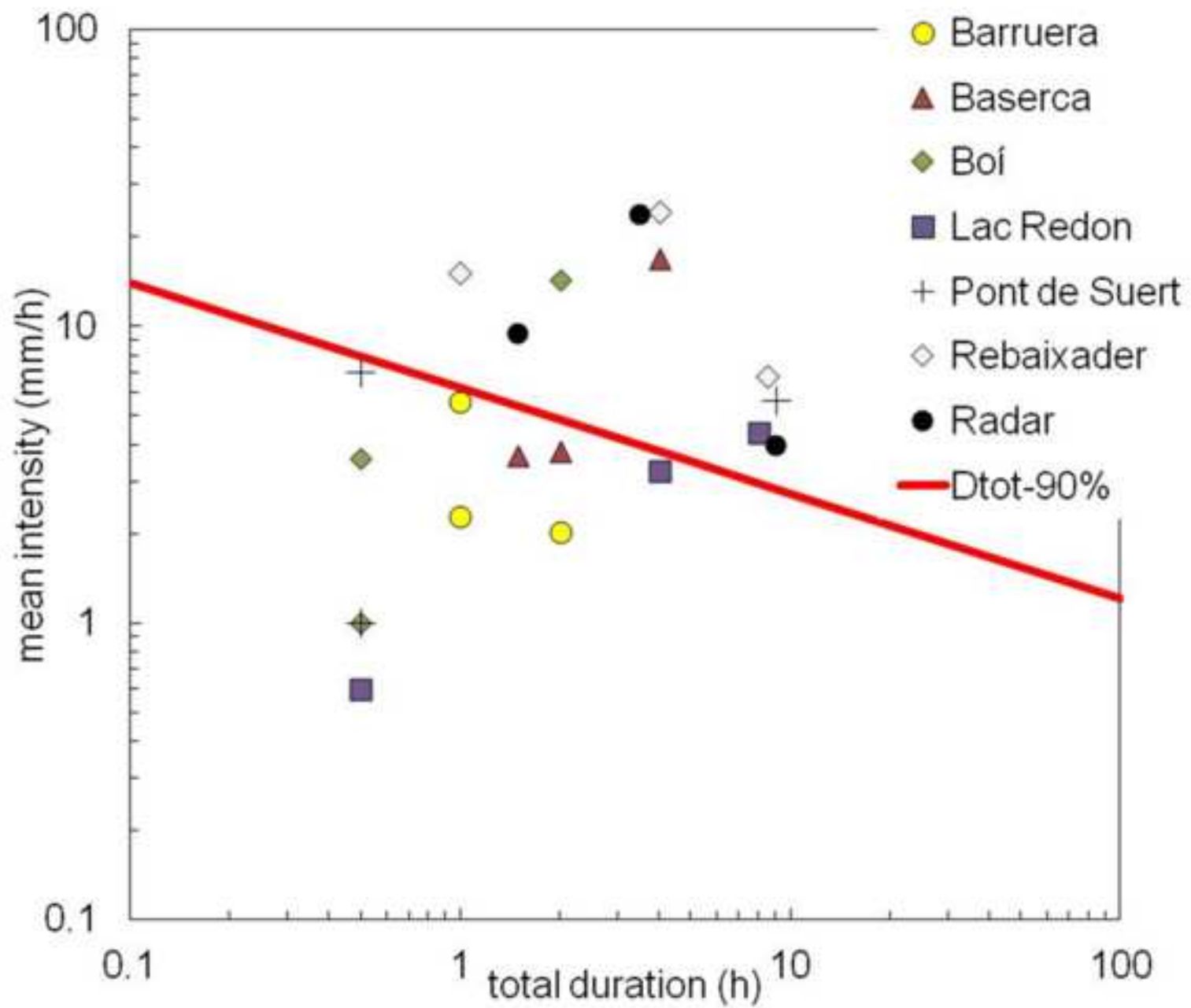












Highlights of the paper (for review):

- Rainfall triggering of 25 torrential flows in a monitored catchment is analysed
- Two different methods for defining rainfall thresholds are applied and compared
- Spatial variability of rainfall is analysed using rain gauges and weather radar for three rainfall events
- Uncertainties in the definition of rainfall thresholds are discussed in detail

ACCEPTED MANUSCRIPT